Iran J Sci Technol Trans Sci (2022) 46:1651–1666
https://doi.org/10.1007/s40995-022-01372-9

RESEARCH PAPER

Dynamical Analysis of COVID-19 Model Incorporating Environmental Factors

Preety Kumari[1,2] · Swarn Singh[4] · Harendra Pal Singh[3]

Received: 23 May 2022 / Accepted: 9 October 2022 / Published online: 28 November 2022
© The Author(s), under exclusive licence to Shiraz University 2022

Abstract

The continuing coronavirus pandemic has come up with considerable questions in front of the world. Presently, India is among concerned countries in Asia. Even though the recovery rate is more than the death rate, it is affecting human lives and experiencing losses to the market. Several methods were employed to study the spread of novel coronavirus. Mathematical modeling is one of the prominent techniques to evaluate the dynamics of novel coronavirus. In this work, we extend the mathematical model SEIAQRDT by incorporating environmental transmission to analyze the transmission of coronavirus in India. The notable aspect of the model incorporates asymptomatic population, quarantine individuals, and environmental transmission factors. These factors have enormous significance in the ongoing COVID-19 outbreak. The basic reproduction number $\boldsymbol{R}_0$ is calculated theoretically. Bifurcation analysis of $\boldsymbol{R}_0$ is also done analytically. The existence and stability analysis of disease-free equilibrium (DFE) and endemic equilibrium (EE) points are established. The impact of environmental factors in spreading COVID-19 pandemic is deliberated. The case study for India and Italy is presented and compared with real data, and the results are in accordance with the real situation.

Keywords Coronavirus · Environment factors · Asymptomatic · Quarantined · Global stability · Bifurcation

1 Introduction

COVID-19 originated in Wuhan, China, in late December 2019 (Wu et al. 2020). In a small-time, the novel coronavirus was transmitted all around the globe. Novel coronavirus disturbs upper respiratory system and causes severe respiratory disease (Oud et al. 2021). COVID-19 was announced as epidemic by WHO (WHO 2020). It is still an ongoing pandemic. Even though the recovery rate is more comparative to death rate, it affects human lives badly. Around 214,766,860 confirmed cases and 4,477,155 deaths were reported by August 26, 2021, in the world (Worldometer 2020a), whereas in India 32,558,530 confirmed and 4,36,396 death cases have been reported (Worldometer 2020b). COVID-19 outbreak surpassed the previous records of diseases like SARS-Cov syndrome (WHO 2020).

The infectious disease has symptoms for instance fever, throat infection, breath shortening, kidney failure, etc. (World Health Organization (WHO) (2021)). The epidemic is continuously transmitting in lack of proper treatment and vaccine doses. The government implemented many preventive measures like social distancing, self-isolation, quarantining, and wearing masks. This disease has presented many challenges in front of scientists and the medical community (Oud et al. 2021). The coronavirus is an extremely communicable disease spread by micro-droplets in the company of symptomatic and asymptomatic infectious individuals or indirect contact with contaminated

✉ Harendra Pal Singh
harendramaths@gmail.com; hpsingh@cic.du.ac.in

Preety Kumari
pkumari@maths.du.ac.in

Swarn Singh
ssingh@svc.ac.in

[1] Faculty of Mathematical Science, University of Delhi, Delhi 110007, India

[2] School of Engineering & Technology, Central University of Haryana, Mahendergarh 123031, India

[3] Cluster Innovation Centre, University of Delhi, Delhi 110007, India

[4] Sri Venkateswara College, University of Delhi, Delhi 110021, India

surfaces (World Health Organization 2020; Gumel et al. 2004; Usaini et al. 2019). The impact of novel coronavirus is transcended compared to other infectious diseases—the primary concern for WHO is the realization of the degree of transmissibility among individuals. The feasibility of being "super-spreaders'' and viable individual-to-individual transmission becomes a matter of concern (World Health Organization 2020; World Health Assembly 2013). According to WHO, super-spreaders are those individuals who spread the disease to more than 20 individuals (World Health Organization 2020).

Mathematical modeling is considered an essential tool in studying novel coronavirus dynamics. Till today, several mathematical models have been employed to assess various factors affecting COVID-19 dynamics (Kizito and Tumwiine 2018). The epistemology model has been conferred in Roosa et al. (2020) which was validated for diseases other than COVID-19 for a shorter period. Generally, the mathematical modeling for COVID-19 is divided into two categories: stochastic and compartmental models. Commonly, compartmental models were used to model infectious diseases (Murray 1993). The popular epidemic models were SIR, SEIR, or SIS (Fu and Milne 2003; Liu et al. 2006; Milne et al. 2008; Pfeifer et al. 2008).

Many other complex mathematical models have been employed for instance SIDARTHE (Giordano et al. 2020) which included the undetected and hospitalized individuals, and SEIAPAHRF (Ndaïrou et al. 2020), which introduces a new compartment, namely super-spreader. These models have taken into account new classes, which help in planning policies for coronavirus (White et al. 2007). Leon et al. (León et al. 2020) developed SEIARD mathematical model to predict state-level outbreaks in Mexico. The parameters for recovery and fatalities were calculated by minimizing the sum of squared errors. Samui et al. (Samui et al. 2020) developed a compartmental model incorporating India's reported and unreported infectious individuals. This model established that the transmission rate for the disease is more beneficial to reduce the basic reproduction number. COVID-19 virus presents challenges day by day. As the virus is new, its mechanism is not yet precise. Krishna and Prakash (Krishna and Prakash 2020) employed the Reservoir-People model for better parameter estimation. A new mathematical model, namely θ-SEIHRD, has been developed by Ivorra et al. (Ivorra et al. 2020). In this model, known characteristics for COVID-19 such as undetected individuals and various sanitary conditions of the hospitalized population have been incorporated. In addition to the undetected population, the fraction θ for detected cases over total cases was introduced (Ivorra et al. 2020). Babaei et al. (Babaei et al. 2021) used fractional derivatives to model dynamics of the epidemic. In particular, this model investigated impact of quarantined individuals on coronavirus outbreaks. Djilali and Ghanbari (Djilali and Ghanbari 2020) studied age-structured model to anticipated outbreak in South Africa, Turkey, and Brazil. As recovery from disease depends on the individual's immune system, it is concluded that old-age people were more affected during the pandemic (Djilali and Ghanbari 2020). The remarkable appearance of diffusion and distribution has been emphasized in the spread of novel coronavirus (Asif et al. 2020). A new hybrid fractional optimal control model was developed for coronavirus epidemic to improve its dynamics (Sweilam et al. 2020). Many real-life problems have been considered in the form of fractional order ODE and PDE in science and engineering (Beghami et al. 2022; Momani et al. 2020a, 2020b; Rabah et al. 2022). Coronavirus is a communicable disorder that can transmit from human to human. Coronavirus mainly spreads in humans during close contact through microdroplets caused by coughing and sneezing (Ji 2020). The literature offers that the spread of coronavirus is also due to contaminated dry surfaces (Dowell et al. 2004; Otter et al. 2016). Role of the environmental transmission is evaluated in few mathematical models. Gralinski and Menachery (Gralinski and Menachery 2020) described that the test conducted from Huanan Seafood Market shows a positive result for COVID-19, which recommends that the virus is transmitted via the environment. During coughing or sneezing of the infectious individual, the virus can transmit in the environment via water droplets. It is also noticed that the virus may present in the environment for many days. Kampf et al. (Kampf et al. 2020) noticed that COVID-19 viruses might survive on inanimate surfaces for up to nine days.

Furthermore, Ong et al. (Ong et al. 2020) described evidence for spread of the virus in the environment via respiratory droplets of coronavirus patients. Thus, it is important to evaluate the effect of environmental transmission in the outbreak of COVID-19. Garba et al. (Garba et al. 2020) studied the impact of environmental factors in novel coronavirus dynamics for South Africa. Alqarni et al. (Alqarni et al. 2020) discussed the effect of environmental contamination in transmission of coronavirus for Saudi Arabia. This paper proposed a new mathematical model by incorporating the environmental factors, requirement rate, and death rate in SEIAQRDT model (Kumari et al. 2021a). The environment transmission factors are considered as in Elmojtaba et al. (2020). This work is arranged as follows: Mathematical model and parameters are conferred in Sect. 2. Section 3 is dedicated to estimating R_0 and stability analysis of DFE point. Section 4 contributes to numerical simulations and discussion. Finally, conclusions are administered in Sect. 5.

2 Model Formulation

We proposed a mathematical model to examine the dynamics of novel coronavirus including asymptomatic, quarantined, and environmental factors by extending the previous model, namely SEIAQRDT (Kumari et al. 2021a). In the proposed model, factors such as requirement rate and natural death rate are also incorporated. In this model, $S(t)$ shows susceptible at time t, $F(t)$ depicts the exposed, $G(t)$ represents the infectious with symptoms, $A(t)$ represents asymptomatic infectious,$Q(t)$ represents the quarantined compartment, $R(t)$ represents the recovered, $H(t)$ represents the dead population, and $T(t)$ represents the protected population. $M(t)$ represents the environmental transmission due to an infected population. The whole population is assumed to be constant. The environmental factor is included in proposed model as $\frac{\beta_e M}{k+M}$. To consider the dynamics of coronavirus, recovery rate $\lambda(t)$ and mortality rate $\kappa(t)$ are expressed as time-dependent functions. The systematic compartmental diagram is given in Fig. 1. This model categorizes the infectious population into symptomatic and asymptomatic individuals. Asymptomatic population are those having no symptoms for the disease, but they can infect others. It is essential to find the asymptomatic population to control spread of disease. Quarantined population considered in this model are total active population for the disease. Model is represented by system of nonlinear differential equations that are characterized as follows:

$$\frac{dS(t)}{dt} = \Lambda - \frac{\beta S(t)(G(t)+q(A(t)))}{N} - \frac{\beta_e S(t)M(t)}{k+M} - (\alpha+\mu)S(t)$$

$$\frac{dF(t)}{dt} = \frac{\beta S(t)(G(t)+q(A(t)))}{N} + \frac{\beta_e S(t)M(t)}{k+M} - (\eta+\mu)F(t)$$

$$\frac{dG(t)}{dt} = p\eta F(t) - (\gamma+\mu+\epsilon)G(t)$$

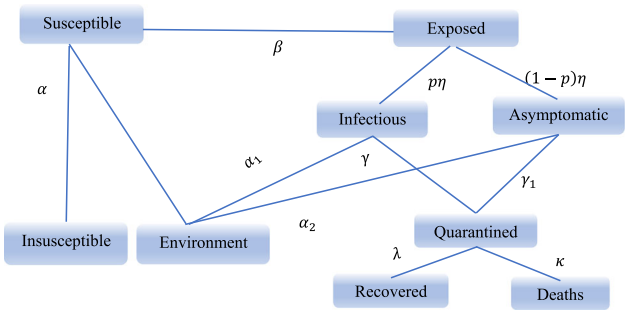

Fig. 1 Compartmental diagram for SEIAQRDT model with environment transmission

$$\frac{dA(t)}{dt} = (1-p)\eta F(t) - (\gamma_1+\mu)A(t)$$

$$\frac{dQ(t)}{dt} = (\gamma+\epsilon)G(t) + \gamma_1 A(t) - \lambda(t)Q(t) - \kappa(t)Q(t) - \mu Q(t)$$

$$\frac{dR(t)}{dt} = \lambda(t)Q(t) - \mu R(t)$$

$$\frac{dH(t)}{dt} = \kappa(t)Q(t) - \mu H(t)$$

$$\frac{dT(t)}{dt} = \alpha S(t) - \mu T(t)$$

$$\frac{dM(t)}{dt} = \alpha_1 G(t) + \alpha_2 A(t) - \mu_e M(t) \quad (2.1)$$

with initial condition $S(0)>0, F(0)\geq 0, G(0)\geq 0, A(0)\geq 0, Q(0)\geq 0, R(0)\geq 0, H(0)\geq 0, T(0)\geq 0, M(0)\geq 0$.

The biological meaning of parameters is described in Table1.

3 Analytical Analyses of the Proposed Model

3.1 Invariant Region

This section determines the invariant region for system (2.1). The non-negativity and boundedness condition is evaluated theoretically.

Lemma 3.1 *Kumari et al. (2021b) If $m'(t)\leq k-gm(t)$ or $m'(t)\geq k-gm(t)$ on the interval (T_1,T_2), where $k, g>0$ and $T_1<T_2$, then*

$$m(t)\leq \frac{k}{g}+\left(m(T_1)-\frac{k}{g}\right)e^{g(T_1-t)} \quad (3.1)$$

$$m(t)\geq \frac{k}{g}+\left(m(T_1)-\frac{k}{g}\right)e^{g(T_1-t)} \quad \forall t\in(T_1,T_2) \quad (3.2)$$

Proposition 3.1 *The solutions of system (2.1) with given initial condition is positively invariant.*

Proof: We prove that the region $(S(t),F(t),G(t),A(t),Q(t),R(t),H(t),T(t))\in\mathbb{R}^8_+$ is positively invariant. For the system (2.1), we get

$$\left.\frac{dS(t)}{dt}\right|_{S=0} = \Lambda > 0 \quad (3.3)$$

Table 1 Parameters and their definition

Symbol	Definition	Symbol	Definition
Λ	Requirement rate	p	Probability of symptomatic infectious
β	Infection rate (symptomatic)	γ	Quarantine rate
α	Protection rate	γ_1	Isolation rate
μ	Natural death/ birth rate	$\lambda(t)$	Recovery rate (time-dependent)
q	Probability of asymptomatic infectious	$\kappa(t)$	Mortality rate (time-dependent)
N	Total population	ϵ	Disease death rate (symptomatic)
β_e	Contact rate from contaminated environment	α_1	Shedding rate from infected (symptomatic) to environment
η	Inverse of average latent time	α_2	Shedding rate from infected (asymptomatic) to environment
k	Concentration of virus at environment	$\frac{1}{\mu_e}$	Lifetime of the virus in the environment

$$\left.\frac{dF(t)}{dt}\right|_{F=0} = \frac{\beta S(t)(G(t)+q(A(t)))}{N} + \frac{\beta_e S(t) M(t)}{k+M} \geq 0 \tag{3.4}$$

$$\left.\frac{dG(t)}{dt}\right|_{I=0} = p\eta F(t) \geq 0 \tag{3.5}$$

$$\left.\frac{dA(t)}{dt}\right|_{A=0} = (1-p)\eta F(t) \geq 0 \tag{3.6}$$

$$\left.\frac{dQ(t)}{dt}\right|_{Q=0} = (\gamma+\epsilon)G(t) + \gamma_1 A(t) \geq 0 \tag{3.7}$$

$$\left.\frac{dR(t)}{dt}\right|_{R=0} = \lambda(t)Q(t) \geq 0 \tag{3.8}$$

$$\left.\frac{dH(t)}{dt}\right|_{H=0} = \kappa(t)Q(t) \geq 0 \tag{3.9}$$

$$\left.\frac{dT(t)}{dt}\right|_{T=0} = \alpha S(t) \geq 0 \tag{3.10}$$

If $(S(0), F(0), G(0), A(0), Q(0), R(0), H(0), T(0)) \in \mathbb{R}^8_+$, then the solution of system (2.1) cannot leave the hyperplane $S=0, F=0, G=0, A=0, Q=0, R=0, H=0, T=0$. Thus, the region $\mathbb{R}^8_+$ is positively invariant.

Theorem 3.1 *System (2.1) describes a dynamical behavior on τ, where*

$\tau = \{(S(t), F(t), G(t), A(t), Q(t), R(t), H(t), T(t)) \in \mathbb{R}^8_+ : N \leq \frac{\Lambda}{\mu}, M(t) \in \mathbb{R}_+ : M(t) \leq \frac{\Lambda}{\mu}\frac{\alpha_1+\alpha_2}{\mu_e}\}$, with the given non-negative initial condition.

Proof: Since $N = S + F + G + A + Q + R + H + T$, therefore $N' = S' + F' + G' + A' + Q' + R' + H' + T'$. We have

$$\frac{dN}{dt} + \mu N \leq \Lambda \tag{3.11}$$

Now, integrating (3.11) and applying the theory of differential equations from (lemma 3.1). We get

$$N \leq \frac{\Lambda}{\mu} + \left(N(T_1) - \frac{\Lambda}{\mu}\right)e^{-\mu t}, \quad \forall t \in (0,\infty) \tag{3.12}$$

for $t \to \infty$, $\left(N(T_1) - \frac{\Lambda}{\mu}\right)e^{-\mu t} \to 0$, which implies $0 < N \leq \frac{\Lambda}{\mu}$.

$M'(t) = \alpha_1 G(t) + \alpha_2 A(t) - \mu_e M(t)$ and $N \leq \frac{\Lambda}{\mu}$.

Therefore, $$\frac{dM}{dt} + \mu_e M \leq \frac{(\alpha_1+\alpha_2)\Lambda}{\mu}. \tag{3.13}$$

By lemma (3.1), we have

$$M \leq \frac{(\alpha_1+\alpha_2)\Lambda}{\mu\mu_e} + \left(M(T_1) - \frac{(\alpha_1+\alpha_2)\Lambda}{\mu\mu_e}\right)e^{-\mu_e t}, \quad \forall\, t \in (0,\infty) \tag{3.14}$$

for $t \to \infty$, $\left(M(T_1) - \frac{(\alpha_1+\alpha_2)\Lambda}{\mu\mu_e}\right)e^{-\mu_e t} \to 0$, which implies $0 \leq M \leq \left(\frac{(\alpha_1+\alpha_2)\Lambda}{\mu\mu_e}\right)$.

Thus, the solution of the system (2.1) lies in $\mathbb{R}^8_+$ and hence possesses a biologically feasible region in τ.

3.2 Basic Reproduction Number (R_0)

R_0 is a parameter in the disease modeling for establishing behavior for the disease. It describes number of secondary infectious through original infectious. The value of R_0 refers to whether the disease will continue or die out in a certain period (Kumari et al. 2021a). There are many methods for the determination of R_0. This article uses the next-generation matrix method for evaluating R_0. For system (2.1), DFE point is calculated by taking left-hand side of system (2.1) equal to zero and considering zero infected individuals. The DFE point for system (2.1) is represented by

$E_1 = \left(\frac{\Lambda}{(\alpha+\mu)}, 0, 0, 0, 0, 0, 0, \frac{\alpha\Lambda}{\mu(\alpha+\mu)}, 0\right)$ and R_0 for the proposed model is equal to $\rho(FV^{-1})$. The transmission matrix $\mathcal{F}$ and v are given as

$$\mathcal{F} = \begin{bmatrix} \frac{\beta S(G+qA)}{N} + \frac{\beta_e SM}{k+M} \\ 0 \\ 0 \\ 0 \end{bmatrix} \text{ and}$$

$$v = \begin{bmatrix} -(\eta+\mu)F \\ p\eta F - (\gamma+\mu+\epsilon)G \\ (1-p)\eta F - (\gamma_1+\mu)A \\ \alpha_1 G + \alpha_2 A - \mu_e M \end{bmatrix}$$

3.3 Local and Global Stability of DFE

The stability analysis of the DFE is discussed here. The local stability of the disease-free equilibrium of the system (2.1) is shown as follows:

Theorem 3.2 *DFE point of system (2.1) is locally asymptotically stable if $R_0 < 1$ otherwise it is unstable.*

Proof: To find local stability of DFE, we compute Jacobian matrix for system (2.1) at E_1 as $J|_{E_1}$

$$J|_{E_1} = \begin{bmatrix} -(\alpha+\mu) & 0 & -\frac{\beta\Lambda}{N(\alpha+\mu)} & \frac{-\beta q\Lambda}{N(\alpha+\mu)} & 0 & 0 & 0 & 0 & \frac{-\beta_e\Lambda}{k(\alpha+\mu)} \\ 0 & -(\eta+\mu) & \frac{\beta\Lambda}{N(\alpha+\mu)} & \frac{\beta\Lambda q}{N(\alpha+\mu)} & 0 & 0 & 0 & 0 & \frac{\beta_e\Lambda}{k(\alpha+\mu)} \\ 0 & p\eta & -(\gamma+\mu+\epsilon) & 0 & 0 & 0 & 0 & 0 & 0 \\ 0 & (1-p)\eta & & -(\gamma_1+\mu) & 0 & 0 & 0 & 0 & 0 \\ 0 & 0 & (\gamma+\epsilon) & \gamma_1 & -(\lambda(t)+\kappa(t)+\mu) & 0 & 0 & 0 & 0 \\ 0 & 0 & 0 & 0 & \lambda(t) & -\mu & 0 & 0 & 0 \\ 0 & 0 & 0 & 0 & \kappa(t) & 0 & -\mu & 0 & 0 \\ 0 & 0 & 0 & 0 & 0 & 0 & 0 & -\mu & 0 \\ 0 & 0 & \alpha_1 & \alpha_2 & 0 & 0 & 0 & 0 & -\mu_e \end{bmatrix}$$

The Jacobian matrices for $\mathcal{F}$ and v at the DFE are given as

$$F = \begin{bmatrix} 0 & \frac{\beta\Lambda}{N(\alpha+\mu)} & \frac{\beta q\Lambda}{N(\alpha+\mu)} & \frac{\beta_e\Lambda}{k(\alpha+\mu)} \\ 0 & 0 & 0 & 0 \\ 0 & 0 & 0 & 0 \\ 0 & 0 & 0 & 0 \end{bmatrix} \text{ and}$$

$$V = \begin{bmatrix} -(\eta+\mu) & 0 & 0 & 0 \\ p\eta & -(\gamma+\mu+\epsilon) & 0 & 0 \\ (1-p)\eta & 0 & -(\gamma_1+\mu) & 0 \\ 0 & \alpha_1 & \alpha_2 & -\mu_e \end{bmatrix},$$

respectively. Thus, the expression for the total basic reproduction number $R_0 = R_h + R_e$ where

$R_h = \frac{\beta p\Lambda\eta}{N(\alpha+\mu)(\gamma+\epsilon+\mu)(\eta+\mu)} + \frac{q\beta\eta\Lambda(1-p)}{N(\alpha+\mu)(\eta+\mu)(\gamma_1+\mu)}$ and $R_e = \frac{\Lambda\beta_e\eta\alpha_2(1-p)}{k(\alpha+\mu)(\eta+\mu)(\mu+\gamma_1)\mu_e} + \frac{\eta\Lambda p\alpha_1\beta_e}{k(\alpha+\mu)(\gamma+\epsilon+\mu)(\eta+\mu)\mu_e}$ represent the term corresponding to individual-to-individual transmission and environment to individual transmission, respectively.

The matrix $J|_{E_1}$ has five negative eigenvalues, namely $\lambda_{1,2,3} = -\mu, \lambda_4 = -\alpha - \mu,$ and $\lambda_5 = -\kappa - \lambda - \mu.$ The remaining four eigenvalues are calculated with the help characteristic equation given as

$$Y^4 + p_1 Y^3 + p_2 Y^2 + p_3 Y + p_4 = 0 \tag{3.15}$$

where

$$p_1 = [\gamma + \epsilon + \eta + 3\mu + \gamma_1 + \mu_e],$$

$$p_2 = \begin{bmatrix} (\gamma+\varepsilon+\mu)(\eta+\mu)(1-R_{h_1}) + (\eta+\mu)(\mu+\gamma_1)(1-R_{h_2}) \\ +(\mu+\gamma_1)(\gamma+\varepsilon+\mu) \\ +(\gamma+\varepsilon+\eta+3\mu+\gamma_1)\mu_e \end{bmatrix}$$

$$p_3 = \begin{bmatrix} (\eta+\mu)(\gamma+\epsilon+\mu)\times \\ \mu_e(1-R_{h_1}-R_{e_1})+(\eta+\mu)(\mu+\gamma_1)\times \\ \mu_e(1-R_{h_2}-R_{e_2})+(\gamma+\epsilon+\mu)(\eta+\mu)(\mu+\gamma_1)\times \\ (1-R_h)+(\gamma+\epsilon+\mu)(\mu+\gamma_1)\mu_e \end{bmatrix},$$

$$p_4 = [(1-R_h-R_e)(\gamma+\epsilon+\mu)(\eta+\mu)(\mu+\gamma_1)\mu_e],$$

$$R_{h_1} = \frac{\beta p\Lambda\eta}{N(\alpha+\mu)(\gamma+\epsilon+\mu)(\eta+\mu)}, R_{h_2} = \frac{q\beta\eta\Lambda(1-p)}{N(\alpha+\mu)(\eta+\mu)(\gamma_1+\mu)},$$

and

$$R_{e_1} = \frac{\Lambda\beta_e\eta\alpha_2(1-p)}{k(\alpha+\mu)(\eta+\mu)(\mu+\gamma_1)\mu_e}, R_{e_2} = \frac{\eta\Lambda p\alpha_1\beta_e}{k(\alpha+\mu)(\gamma+\epsilon+\mu)(\eta+\mu)\mu_e}.$$

To discuss the stability of system (2.1), we employ the Routh–Hurwitz criterion. To prove that roots of equation (3.15) have negative real parts, the following conditions need to be satisfied:

(1) $p_1, p_2, p_3, p_4 > 0$. Since all the coefficients of equation (3.15) are positive, whenever $R_h + R_e < 1$ *i.e.*, $R_0 < 1$. Therefore, the condition is satisfied.

(2) $p_1p_2p_3 > p_3^2 + p_1^2p_4$. To prove this, we begin with the term $p_1p_2 - p_3$

$$p_1p_2 - p_3 = (\gamma+\epsilon+3\mu+\eta+\gamma_1+\mu_e)\begin{bmatrix}(\gamma+\epsilon+\mu)(\eta+\mu)(1-R_{h1})+(\eta+\mu)(\mu+\gamma_1)(1-R_{h2}) \\ +(\mu+\gamma_1)(\gamma+\epsilon+\mu)+(\gamma+\epsilon+\eta+3\mu+\gamma_1)\mu_e)\end{bmatrix}$$
$$-\begin{bmatrix}(\eta+\mu)(\gamma+\epsilon+\mu)\mu_e(1-R_{h_1}-R_{e_1})+(\eta+\mu)(\mu+\gamma_1)\mu_e(1-R_{h_2}-R_{e_2}) \\ +(\gamma+\epsilon+\mu)(\eta+\mu)(\mu+\gamma_1)(1-R_h)+(\gamma+\epsilon+\mu)(\mu+\gamma_1)\mu_e\end{bmatrix}$$

$$=(\gamma+\epsilon+3\mu+\eta+\gamma_1)$$
$$\begin{bmatrix}(\gamma+\epsilon+\mu)(\eta+\mu)(1-R_{h1})+(\eta+\mu)(\mu+\gamma_1)(1-R_{h2}) \\ +(\mu+\gamma_1)(\gamma+\epsilon+\mu)+(\gamma+\epsilon+\eta+3\mu+\gamma_1)\mu_e)\end{bmatrix}$$
$$+\mu_e\begin{bmatrix}(\gamma+\epsilon+\mu)(\eta+\mu)(1-R_{h1})+(\eta+\mu)(\mu+\gamma_1)(1-R_{h2}) \\ +(\mu+\gamma_1)(\gamma+\epsilon+\mu)+(\gamma+\epsilon+\eta+3\mu+\gamma_1)\mu_e)\end{bmatrix}$$
$$-\mu_e\begin{bmatrix}(\eta+\mu)(\gamma+\epsilon+\mu)(1-R_{h_1})-R_{e_1}(\gamma+\epsilon+\mu)(\eta+\mu) \\ +(\eta+\mu)(\mu+\gamma_1)(1-R_{h_2})+R_{e2}(\eta+\mu)(\mu+\gamma_1)+(\gamma+\epsilon+\mu)(\mu+\gamma_1)\end{bmatrix}$$
$$-(\gamma+\epsilon+\mu)(\eta+\mu)(\mu+\gamma_1)(1-R_{h1})+(\gamma+\epsilon+\mu)(\eta+\mu)(\mu+\gamma_1)R_{h2}$$

$$=(\gamma+\epsilon+3\mu+\eta+\gamma_1)$$
$$\begin{bmatrix}(\gamma+\epsilon+\mu)(\eta+\mu)(1-R_{h1})+(\eta+\mu)(\mu+\gamma_1)(1-R_{h2}) \\ +(\mu+\gamma_1)(\gamma+\epsilon+\mu)+(\gamma+\epsilon+\eta+3\mu+\gamma_1)\mu_e)\end{bmatrix}$$
$$+\mu_e[(\gamma+\epsilon+\eta+3\mu+\gamma_1)\mu_e)]$$
$$-\mu_e[-R_{e_1}(\gamma+\epsilon+\mu)(\eta+\mu)-R_{e2}(\eta+\mu)(\mu+\gamma_1)]$$
$$+(\gamma+\epsilon+\mu)(\eta+\mu)(\mu+\gamma_1)R_{h2}$$

$$=(\gamma+\epsilon+3\mu+\eta+\gamma_1)$$
$$[(\gamma+\epsilon+\mu)(\eta+\mu)(1-R_{h1})+(\eta+\mu)(\mu+\gamma_1)(1-R_{h2})]$$
$$+[R_{e_1}(\gamma+\epsilon+\mu)(\eta+\mu)\mu_e+R_{e2}(\eta+\mu)(\mu+\gamma_1)\mu_e$$
$$+(\gamma+\epsilon+\mu)(\eta+\mu)(\mu+\gamma_1)R_{h2}(\gamma+\epsilon+\eta+3\mu+\gamma_1)$$
$$\left[(\gamma+\epsilon+\mu)(\mu+\gamma_1)+\mu_e(\gamma+\epsilon+\eta+3\mu+\gamma_1)+\mu_e^2\right]$$

It is clear that $(p_1p_2 - p_3) > 0$ if $R_{h1} < 1$ and $R_{h2} < 1$, which is true whenever $R_0 < 1$.

According to the Routh–Hurwitz criteria, $p_1p_2 > p_3$ is also a condition for the characteristic equation of degree four. Thus, we have

$$
\begin{aligned}
&p_1p_2p_3 - p_3^2 - p_1^2p_4 \\
&= (p_1p_2 - p_3)p_3 - p_1^2p_4 \\
&= (\gamma + \epsilon + 3\mu + \eta + \gamma_1) \\
&[(\gamma + \epsilon + \mu)(\eta + \mu)(1 - R_{h1}) + (\eta + \mu)(\mu + \gamma_1)(1 - R_{h2})] \\
&+ [R_{e_1}(\gamma + \epsilon + \mu)(\eta + \mu)\mu_e + R_{e2}(\eta + \mu)(\mu + \gamma_1)\mu_e \\
&+ (\gamma + \epsilon + \mu)(\eta + \mu)(\mu + \gamma_1)R_{h2}] + (\gamma + \epsilon + \eta + 3\mu + \gamma_1) \\
&\left[(\gamma + \epsilon + \mu)(\mu + \gamma_1) + \mu_e(\gamma + \epsilon + \eta + 3\mu + \gamma_1) + \mu_e^2\right] \\
&\times \begin{bmatrix} (\eta + \mu)(\gamma + \epsilon + \mu)\mu_e(1 - R_{h_1} - R_{e_1}) + (\eta + \mu)(\mu + \gamma_1)\mu_e(1 - R_{h_2} - R_{e_2}) \\ +(\gamma + \epsilon + \mu)(\eta + \mu)(\mu + \gamma_1)(1 - R_h) + (\gamma + \epsilon + \mu)(\mu + \gamma_1)\mu_e \end{bmatrix} \\
&- (\gamma + \epsilon + 3\mu + \eta + \gamma_1 + \mu_e)^2(\gamma + \epsilon + \mu)(\eta + \mu)(\mu + \gamma_1)\mu_e(1 - R_h - R_e) \\
&= \begin{pmatrix} \gamma^2 + \epsilon^2 + 9\mu^2 + \eta^2 + \gamma_1^2 + \mu_e^2 + 2\gamma\epsilon \\ +6\epsilon\mu + 6\gamma\mu + 2\eta\mu_e + 2\mu_e\gamma_1 + \eta\gamma_1 + 2\gamma\eta + 2\gamma\mu_e \\ + 2\gamma\gamma_1 + 2\epsilon\eta + 2\epsilon\mu_e + 2\epsilon\gamma_1 + 6\mu\eta + 6\mu\mu_e + 6\mu\gamma_1 \end{pmatrix} \\
&(\gamma + \epsilon + \mu)(\eta + \mu)(\mu + \gamma_1)\mu_e + (+ve) \text{ terms} \\
&= (\gamma + \epsilon + 3\mu + \eta + \gamma_1 + \mu_e)^2 \\
&(\gamma + \epsilon + \mu)(\eta + \mu)(\mu + \gamma_1)\mu_e(R_h + R_e) + (+ve) \text{ terms}
\end{aligned}
$$

This implies the condition $p_1p_2p_3 > p_3^2 + p_1^2p_4$ is satisfied. Therefore, system (2.1) is locally asymptomatically stable about DFE if $R_0 < 1$.

Moreover, the global stability of DFE is proved in the following theorem:

Theorem 3.3 *DFE of system* (2.1) *is globally asymptomatically stable if* $R_0 < 1$ *and the condition* (1) and condition (2) are satisfied:

(1) $\frac{dU}{dt} = J(U, 0), U_0$ is global asymptotically stable.
(2) $\hat{K}(U, V) \geq 0$ for $(U, V) \in \tau$.

where $\widehat{K}(U, V) = AV - K(U, V)$, $A = D_V K(U_0, 0)$ is M-matrix and

$\tau = \{(S(t), F(t), G(t), A(t), Q(t), R(t), H(t), T(t)) \in \mathbb{R}_+^8 : N \leq \frac{\Lambda}{\mu}, M(t) \in \mathbb{R}_+ : M(t) \leq \frac{\Lambda}{\mu}\frac{\alpha_1 + \alpha_2}{\mu_e}\}$ is the biologically feasible region.

Proof: Global stability of the system (2.1) is established by employing theorem of Feng et al. (Castillo-Chavez et al. 2002). System (2.1) is written in the form as follows:

$\frac{dU}{dt} = J(U, V)$, $\frac{dV}{dt} = K(U, V)$ and $K(U, 0) = 0$ where $U = (S, Q, R, H, T)$ and $V = (F, G, A, M)$ are non-infected and infected compartments, respectively. $J(U, V)$ and $K(U, V)$ represent right-hand side of the system (2.1) corresponding to U and$V$, respectively. DFE is written as $E_1 = (U_0, 0)$ where $U_0 = \left(\frac{\Lambda}{(\alpha+\mu)}, 0, 0, 0, \frac{\alpha\Lambda}{\mu(\alpha+\mu)}\right)$.

To prove condition 1), we have

$$
\begin{bmatrix} S' \\ Q' \\ R' \\ H' \\ T' \end{bmatrix} = \begin{bmatrix} \Lambda - (\alpha + \mu)S \\ -\lambda Q - \kappa Q - \mu Q \\ -\mu R \\ -\mu H \\ \alpha S - \mu T \end{bmatrix}
$$

solving the above differential equations, we have:

$$
\begin{aligned}
S(t) &= C_1e^{-(\alpha+\mu)t} + \frac{\Lambda}{(\alpha + \mu)}, Q(t) = C_2e^{-(\lambda+\kappa+\mu)t}, R(t) \\
&= C_3e^{-\mu t}, H(t) = C_4e^{-\mu t}, \\
T(t) &= \alpha\left(\frac{\Lambda}{(\alpha + \mu)}\right) - \frac{C_1}{\alpha}e^{-(\alpha+\mu)t} + C_5e^{-\mu t},
\end{aligned}
$$

where C_1, C_2, C_3, C_4, and C_5 are arbitrary constants. Since $U \to U_0$ as $t \to \infty$. Therefore, U_0 is globally

asymptotically stable, hence condition (1) is satisfied. Now to show condition(2), we have matrix A :

$$A = \begin{bmatrix} -(\eta+\mu) & \frac{\beta\Lambda}{N(\alpha+\mu)} & \frac{\beta\Lambda q}{N(\alpha+\mu)} & \frac{\beta_e\Lambda}{k(\alpha+\mu)} \\ p\eta & -(\gamma+\mu+\epsilon) & 0 & 0 \\ (1-p)\eta & 0 & -(\gamma_1+\mu) & 0 \\ 0 & \alpha_1 & \alpha_2 & -\mu_e \end{bmatrix}.$$

$$\hat{K}(U,V) = AV - K(U,V) = \begin{bmatrix} \frac{\beta G}{N}\left(\frac{\Lambda}{\alpha+\mu} - S\right) + \frac{\beta qA}{N}\left(\frac{\Lambda}{\alpha+\mu} - S\right) + \frac{\beta_e M}{(k+M)}\left[\frac{M\Lambda}{k(\alpha+\mu)} + \left(\frac{\Lambda}{\alpha+\mu} - S\right)\right] \\ 0 \\ 0 \\ 0 \end{bmatrix}$$

Now, we obtain

Clearly, $\hat{K}(U,V) \geq 0 \forall (U,V) \in \tau$. Hence DFE is global stable.

3.4 Existence and Stability of EE

Existence and local stability of the EE point are discussed here. To find EE for system (2.1), we assume $E_2 = (S^*, F^*, G^*, A^*, Q^*, R^*, H^*, T^*, M^*)$ to be endemic equilibrium.

We define the following:

$$\Psi = \frac{\beta(G^* + qA^*)}{N} + \frac{\beta_e M^*}{(k+M^*)}. \tag{3.16}$$

Now, the endemic equilibrium is calculated by substituting left-hand side of system (2.1) equal to zero. The EE point for system (2.1) is written as

$$\begin{cases} S^* = \frac{\Lambda}{\Psi + (\alpha+\mu)}, & F^* = \frac{\Psi S^*}{(\eta+\mu)}, & G^* = \frac{p\eta F^*}{(\gamma+\epsilon+\mu)}, \\ A^* = \frac{(1-p)\eta F^*}{(\gamma_1+\mu)}, & Q^* = \frac{(\gamma+\epsilon)G^* + \gamma_1 A^*}{(\lambda+\kappa+\mu)}, & R^* = \frac{\lambda Q^*}{\mu}, \\ H^* = \frac{\kappa Q^*}{\mu}, & T^* = \frac{\alpha S^*}{\mu}, & M^* = \frac{\alpha_1 G^* + \alpha_2 A^*}{\mu_e} \end{cases} \tag{3.17}$$

Substituting the values of expression (3.17) in Eq. (3.16), we have

$$q_1\Psi^2 + q_2\Psi + q_3 = 0 \tag{3.18}$$

where

$$q_1 = N(\gamma+\epsilon+\mu)(\eta+\mu)(\mu+\gamma_1) \left(k(\gamma+\epsilon+\mu)(\eta+\mu)(\mu+\gamma_1) + \Lambda(\alpha_1\rho\eta(\mu+\gamma_1) + \alpha_2(1-\rho)\eta(\gamma+\epsilon+\mu)\right),$$

$$\begin{aligned} q_2 =& Nk\mu_e(\gamma+\epsilon+\mu)^2 \\ & (\eta+\mu)^2(\mu+\gamma_1)^2(\alpha+\mu)(1-R_h-R_e) \\ & + N(\gamma+\epsilon+\mu)(\eta+\mu)(\mu+\gamma_1)(\alpha+\mu) \\ & \Lambda(\alpha_1\rho\eta(\mu+\gamma_1) + \alpha_2(1-\rho)\eta(\gamma+\epsilon+\mu) \\ & + Nk\mu_e(\gamma+\epsilon+\mu)^2(\eta+\mu)^2(\mu+\gamma_1)^2(\alpha+\mu), \end{aligned}$$

$$q_3 = Nk\mu_e(\gamma+\epsilon+\mu)^2(\eta+\mu)^2(\mu+\gamma_1)^2(\alpha+\mu)^2(1-R_h-R_e).$$

It is noticed that $q_1 > 0$. The endemic equilibrium exists if Eq. (3.18) has a positive solution. The following cases are given below:

(1) If $R_0 = R_h + R_e \leq 1$, then all the coefficients of Eq. (3.18) are greater than or equal to zero. In this case, Eq. (3.18) has no positive solution, and hence no endemic equilibrium exists.

(2) If $R_0 = R_h + R_e > 1$, then $q_3 < 0$. Thus, Eq. (3.18) has unique positive solution, and hence a unique endemic equilibrium (EE) exists.

Theorem 3.4. *The EE of system (2.1) is locally asymptomatically stable if $R_0 > 1$.*

Proof: Stability of EE is proved using condition described in Castillo-Chavez and Song (2004). Let β_e be a bifurcation parameter. Then, the value of the bifurcation parameter at $R_0 = 1$ is given as.

$$\beta_e^c = \frac{k\mu_e(N(\gamma+\epsilon+\mu)(\eta+\mu)(\mu+\gamma_1)(\alpha+\mu) - \beta\eta\Lambda(p(\mu+\gamma_1) + q(1-p)(\gamma+\epsilon+\mu)))}{N\eta\Lambda(\alpha_1 p(\gamma_1+\mu) + \alpha_2(1-p)(\gamma+\epsilon+\mu))}$$

Table 2 Parameter values for India

α	0.0087 [fitted]	β_e	0.0000012 (Oud et al. 2021)
β	1.4783 [fitted]	q	$2.76 * 10^{-5}$[fitted]
η	0.2806 [fitted]	α_1	0.2157 (Oud et al. 2021)
γ	0.4294 [fitted]	α_2, μ_e	0.2276 (Oud et al. 2021)
p	0.6900 [fitted]	$\lambda(1)$	0.1118 [fitted]
γ_1	0.5394 [fitted]	$\lambda(2)$	0.0685 [fitted]
k	0.2 [0,1] (Elmojtaba et al. 2020)	$\lambda(3)$	0.0141 [fitted]
ϵ	0.1814 [fitted]	$\kappa(1)$	0.0027 [fitted]
Λ	0.0154 [assumed]	$\kappa(2)$	0.0249 [fitted]
μ	0.0004 (Oud et al. 2021)	$\kappa(3)$	96.1418 [fitted]

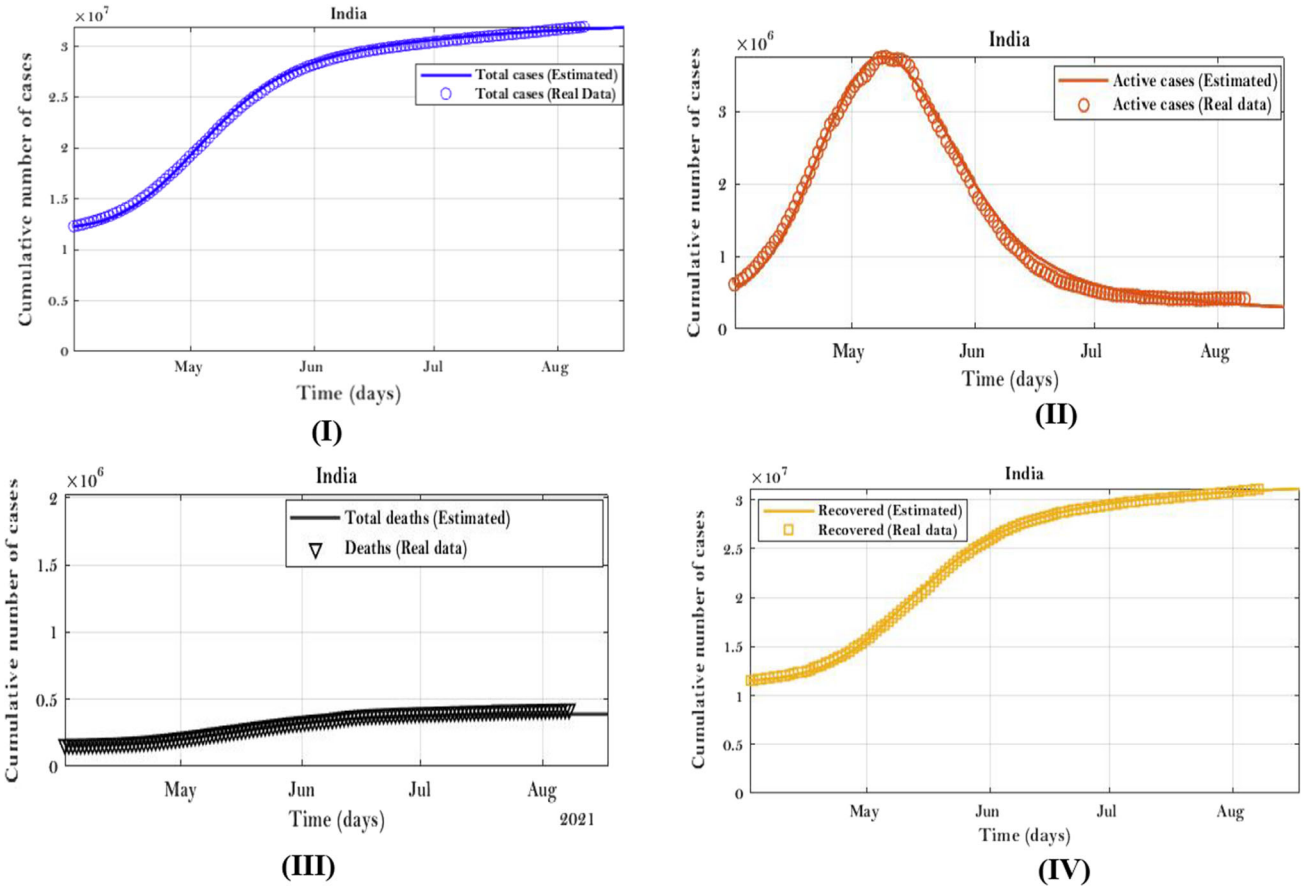

Fig. 2 Fitting of cumulative (confirmed, recovered, deaths and active cases) for real data India. The markers circle and triangle represent the real data and solid lines represent the simulated cases for the proposed model

The Jacobian matrix $J|_{E1}$ has a zero eigenvalue at $R_0 = 1$. As one of the eigenvalues is zero, there is a chance of bifurcation.

Let $A = [a_1 a_2 \cdots a_9]$ and $B = [b_1 b_2 \cdots b_9]$ denote the left and right eigenvector with respect to zero eigenvalue, respectively. Where

$$a_1 = a_5 = a_6 = a_7 = a_8 = 0$$

$$a_2 = \frac{k(\alpha+\mu)\mu_e}{\Lambda\beta_e^c} a_9, a_3 = \frac{\beta\Lambda}{N(\gamma+\epsilon+\mu)(\alpha+\mu)} a_2 + \frac{\alpha_1}{(\gamma+\epsilon+\mu)} a_9$$

Table 3 Parameters of numerical simulation for Italy

α	0.1007 [fitted]	β_e	0.0000012 (Oud et al. 2021)
β	1.6973 [fitted]	q	0.1 [fitted]
η	0.0160 [fitted]	α_1	0.2157 (Oud et al. 2021)
γ	0.1746 [fitted]	α_2, μ_e	0.2276 (Oud et al. 2021)
p	0.30 [fitted]	$\lambda(1)$	0.0754 [fitted]
γ_1	0.25 [fitted]	$\lambda(2)$	0.0384 [fitted]
k	0.2 [0,1] (Elmojtaba et al. 2020)	$\lambda(3)$	8.7637 [fitted]
ϵ	0.034 (Oud et al. 2021)	$\kappa(1)$	0.0011 [fitted]
Λ	0.589 [assumed]	$\kappa(2)$	0.0049 [fitted]
μ	0.00107 [assumed]	$\kappa(3)$	8.2450 [fitted]

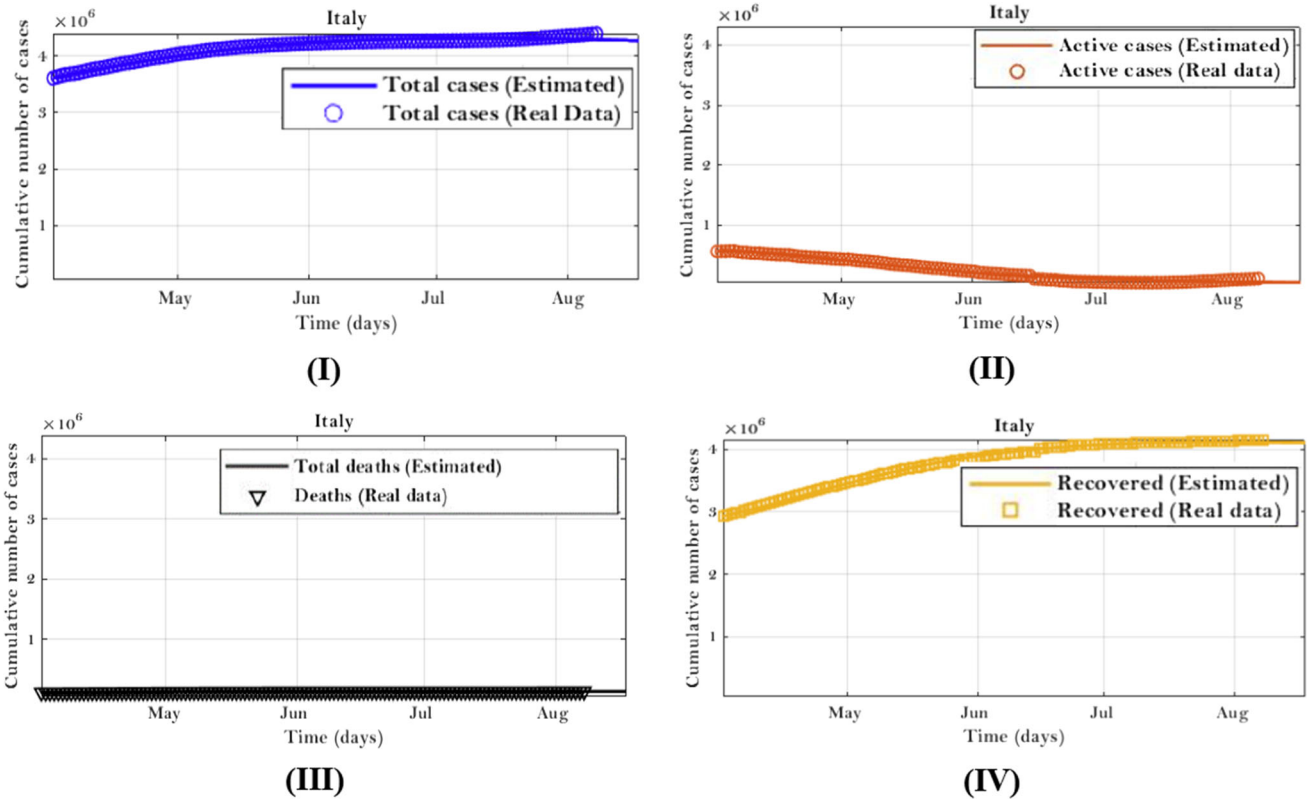

Fig. 3 Fitting of cumulative (confirmed, recovered, deaths and active cases) for real data Italy. The markers circle and triangle represent the real data and solid lines represent the simulated cases for the proposed model.

$$a_4 = \frac{\alpha_2}{(\gamma_1+\mu)}a_9 + \frac{q\beta\Lambda}{N(\alpha+\mu)(\gamma+\epsilon+\mu)}a_2, a_9 = a_9 \neq 0$$

$$b_1 = \frac{-(\eta+\mu)}{(\alpha+\mu)}b_2, b_2 = b_2 \neq 0, b_3 = \frac{\eta p}{(\gamma+\epsilon+\mu)}b_2$$

$$b_4 = \frac{(1-p)\eta}{(\gamma_1+\mu)}b_2, b_5 = \frac{(\gamma+\epsilon)b_3+\gamma_1 b_4}{(\kappa+\lambda+\mu)}, b_6 = \frac{\lambda}{\mu}b_5$$

$$b_7 = \frac{\kappa}{\mu}b_5, b_8 = \frac{\alpha}{\mu}b_1, b_9 = \frac{\alpha_1 b_3+\alpha_2 b_4}{\mu_e}$$

Now, assuming free variables a_2 and b_9 to be $+ve$ and finding values of a and b (Castillo-Chavez and Song 2004). We find that $a<0$ and $b>0$. Therefore, the bifurcation is in forward direction. Hence, EE is locally asymptomatically stable whenever $R_0 > 1$.

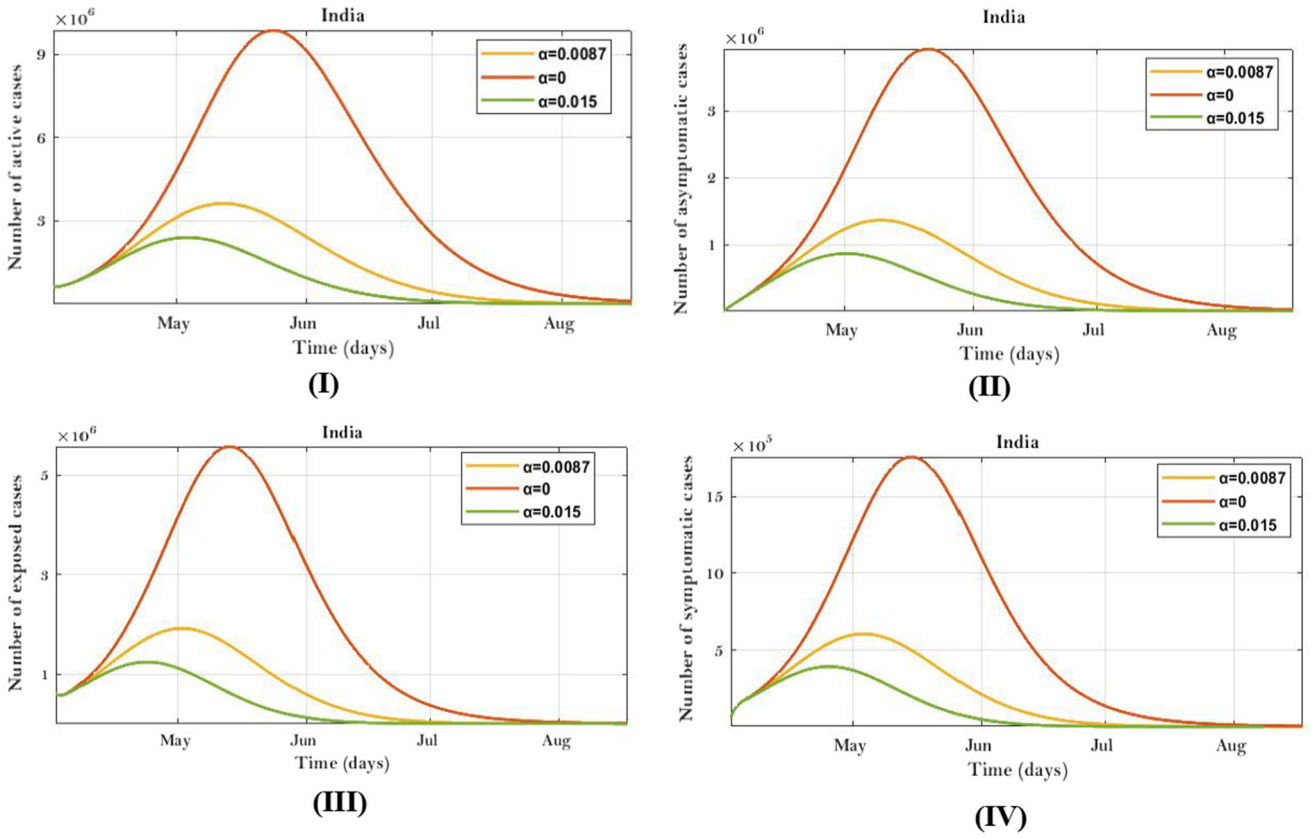

Fig. 4 Results of system (2.1), reveal the decrease in the infectious population as the protection rate α increases: **I** active or quarantined, **II** asymptomatic, **III** exposed, and **IV** symptomatic population, respectively for distinct values of α.

4 Numerical Simulation & Discussion

Nowadays one of the questions in each individual mind is 'will this disease ever die out?'. The experts recommend that in the current situation its disappearance is mostly unlikely: 'COVID-19 spread in individuals very easily by direct contact or contaminated areas' (Gunia and Will, 2020). Therefore, a country like India with a dense population is worried about the future wave. According to WHO officials, COVID-19 may behave in a periodical manner and we need to deal with it (Gunia and Will, 2020). From the above discussion, we may conclude as (Yang and Wang 2020), we need to do the complete quantitative and qualitative analysis of proposed model. Therefore, this section presents numerical simulations of system (2.1) for India and Italy. In simulation, we consider the effect of protection rate and environment factors. Fitting of parameters has been done by employing the real data for India and Italy to anticipate the spread of epidemic. Next subsection deals with the estimation of parameters using the data for India (Covid19 India 2021).

4.1 Simulation Results for India

Parameters are fitted by the real cases for India (confirmed, active, recovered, and deaths). Comparison of real data for India with the predicated cases is done from April 01, 2021, to August 08, 2021. The fitted model presents satisfactory results up to August 08, 2021. Parameters for simulation are shown in Table 2.

In this model, the recovery rate $(\lambda(t))$ and death rate $(\kappa(t))$ are dependent functions of time given as follows (Cheynet 2020):

$$\lambda(t) = \frac{\lambda(1)}{1 + e^{(-\lambda(2)*(t-\lambda(3))}}, \kappa(t) = \frac{\kappa(1)}{(e^{(\kappa(2)*(t-\kappa(3))} + e^{-\kappa(2)*(t-\kappa(3))})}$$

where $\lambda(1), \lambda(2), \lambda(3), \kappa(1), \kappa(2),$ and$\kappa(3)$ are fitted parameters specified in Table 2. The parameters are optimized using lsqcurvefit function in MATLAB (Kumari et al. 2021a). Figure 2 I–IV shows the fitted curve for cumulative (total, active, deaths, and recovered) cases in India. Results reveal the agreement between real data and model predicted data. To evaluate the accuracy of data fitted, we find the NRMSE (normalized root mean square

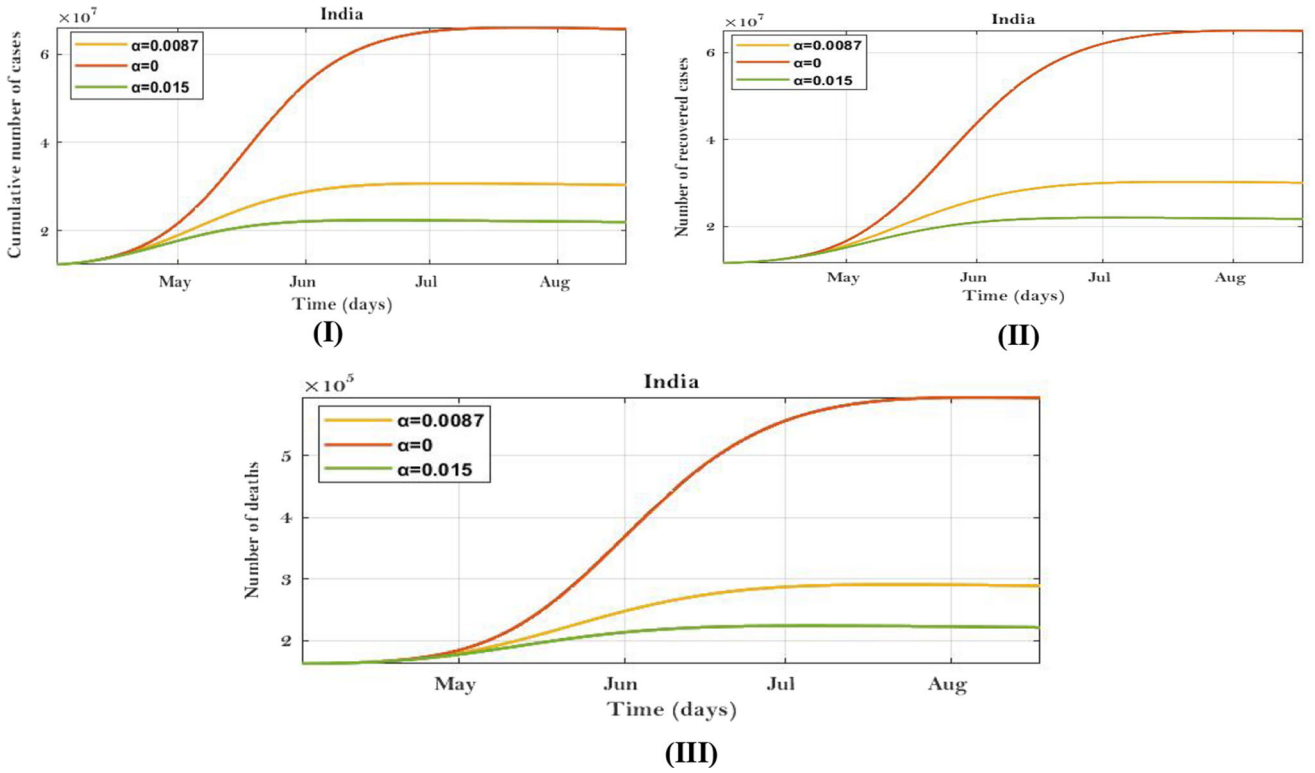

Fig. 5 The cumulative deaths drastically increases when there is no control measure i.e., $\alpha = 0$, total numbers of cases I, recovery **II**, and deaths **III** decreases as α increases, for distinct values of α

error). The formula for NRMSE is commonly defined as follows:

$$\text{NRMSE} = \frac{\sqrt{\sum_{j=1}^{n}(y_j - z_j)^2}}{\sum_{j=1}^{n} z_j}, \quad \text{where} \quad z_j(1 \le j \le n) \quad \text{and}$$

$y_j(1 \le j \le n)$ are real data for India and predicted data by the proposed model, respectively. n is the number of days under consideration. We found that NRSME for the proposed model for India is 0.0075. Moreover, Karl Pearson's correlation coefficient is 0.99. The above analysis shows that the proposed model is a good fit with real data.

4.2 Simulation Results for Italy

Parameters are also fitted by real data for Italy (confirmed, active, recovered, and death cases). The comparison of real data for Italy with the predicated data is done from April 01, 2021, to August 08, 2021. The fitted model presents satisfactory results up to August 08, 2021. The estimated parameters are shown in Table 3. Figure 3 I–IV represents fitted curve for cumulative (confirmed, active, death, and recovered) cases for Italy. It is observed from the figures that simulated data are in good agreement with real data.

4.3 Impact of Protection Rate on COVID-19

This subsection deals with the simulation results and the analysis accomplished by applying the novel coronavirus data for India to evaluate the potential impact of control strategies. The effect of preventive measures such as social distancing, isolation and quarantined are estimated through the simulation of system (2.1) using parameters from Table 2. The results reveal decrease in number of exposed, symptomatic, asymptomatic, and quarantined (active) cases with increase in parameter α as illustrated in Fig. 4 I, II, III, IV, respectively. The results are in correspondence with the fact that as control strategies decline the number of infectious increases (Ngonghala et al. 2020).

Figure 4 I, II, III, IV recommends that if strict control measures were used ($\alpha = 0.015$ instead of $\alpha = 0.0087$), then the number of cases was quite less. If the protection rate is 0.015, then total cases are expected to be 19,220,000 on May 07, 2021. In this case, peak for the second wave was attained as depicted in Fig. 5I. On the other hand, if the protection rate is relaxed to 0.0087, then the total confirmed cases at peak of pandemic was reached 21,580,000 as shown in Fig. 5I. Figure 5I, II, III presents cumulative (confirmed, recovered, and death) cases. Fig. 5I, II, III reveals decrease in confirmed cases, recoveries, and deaths, respectively, whenever the protection rate

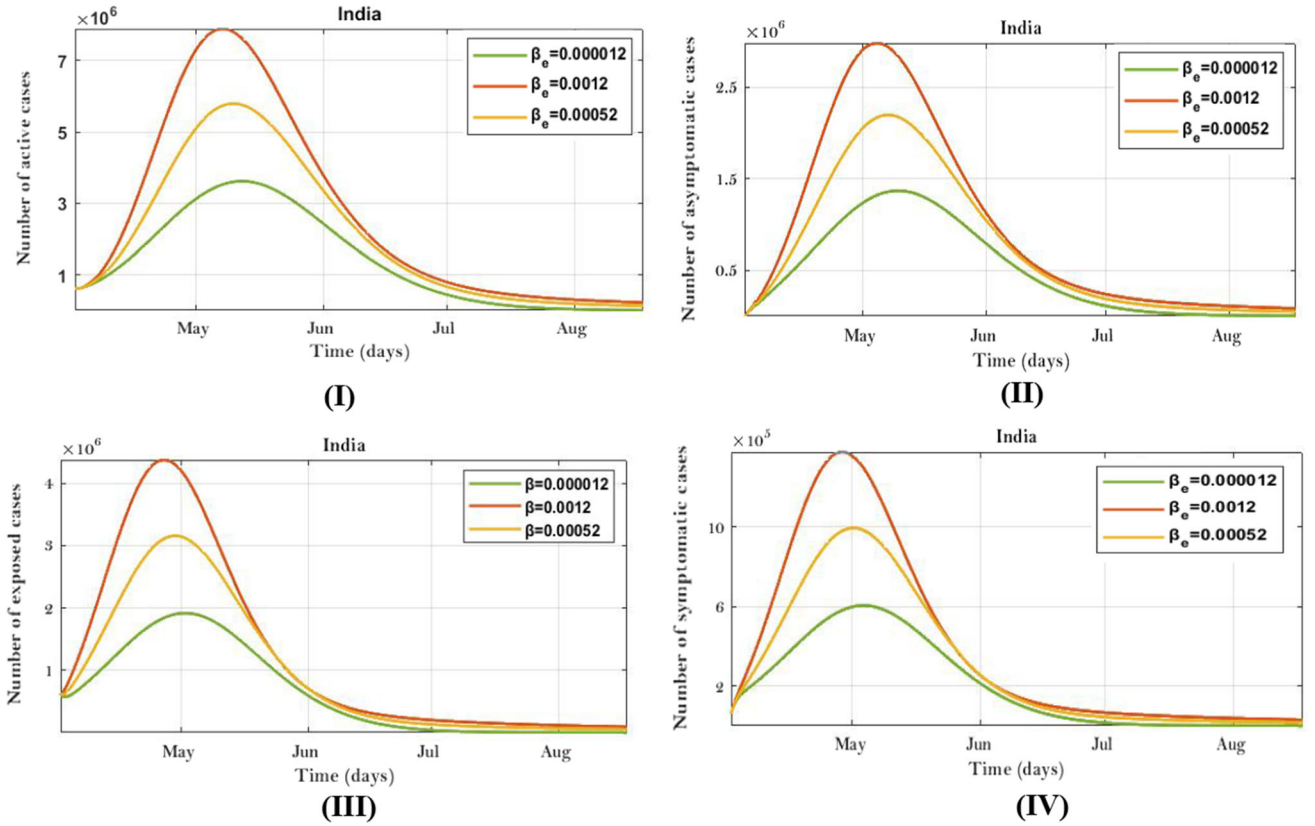

Fig. 6 Results of the system (2.1), revealing the increase in the infectious population as the contact rate from contaminated environment (β_e) increases: **a** active or quarantined, **b** asymptomatic, **c** exposed, and **d** symptomatic population, respectively, for distinct values of β_e

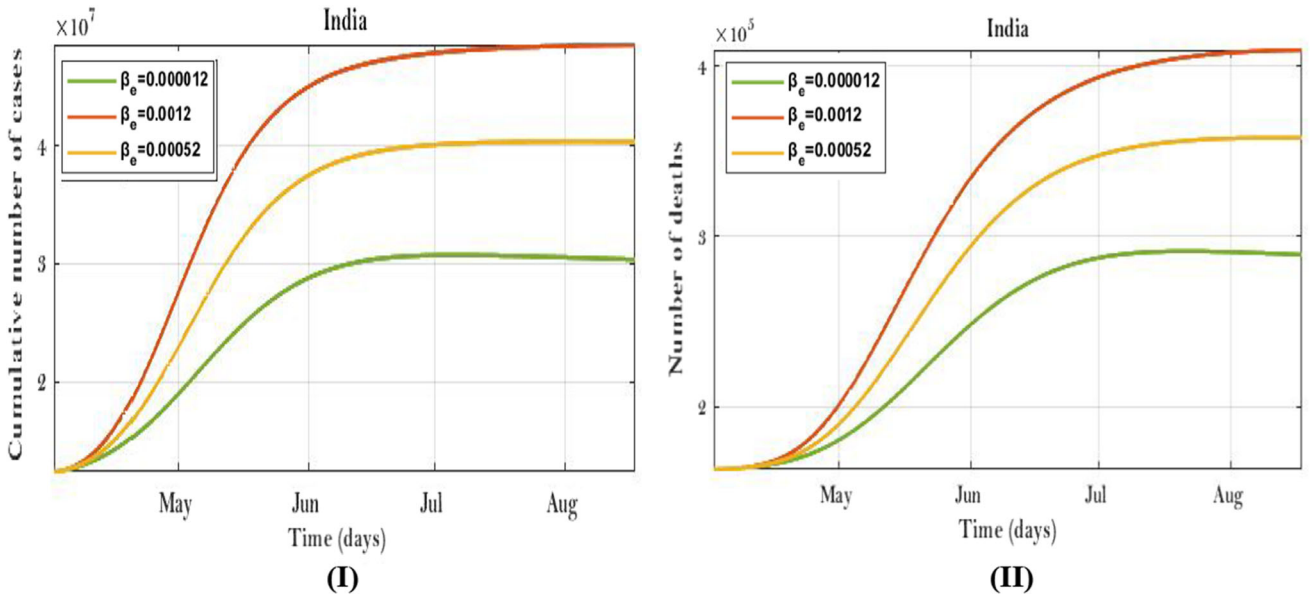

Fig. 7 The cumulative deaths increases when there is increase in the parameter β_e, total numbers of cases **a** and deaths **b** increases as β_e increases, for distinct values of β_e

increases. It also discusses the case when no protection was present, i.e., $\alpha = 0$. It will show a drastic increase in the number of deaths with time. Therefore, these results reveal that the implementation of strict control strategies like lockdown imposed by the central government of India has a notable impact on the spread of novel coronavirus.

Furthermore, the above discussion suggests that the lockdown imposed in India for the first time on March 23, 2020 is unlocked in a phased manner. Thereafter, strict control measures are again implemented in May 2021 which are also going to be uplifted in a phased manner. The major challenge is that the uplifting of lockdown may not disturb the control of the epidemic seen after the second wave in India. Hence, the current study strongly recommends that preventive measures like social distancing, wearing of masks, etc., must be taken care of so that we can avoid the recurrence of the epidemic. In the literature, it is shown that countries such as South Korea and Hong Kong have relaxed preventive measures and facing the recurrence of the disease (Rogers 2020).

4.4 Impact of Environmental Transmission

As indicated before, it is an extensively used drive that the virus survives on the contaminated surfaces for many days on distinct surfaces (Seladi-Schulman 2020). The COVID-19 virus can continue to live on the contaminated areas for up to 9 days (Kampf et al. 2020). In particular, the crowded places like slum areas where many people live in a very small region can easily come in contact with such surfaces after water droplets from the infected person arrive on them. Therefore, it is not uncertain that the novel coronavirus pandemic in India has an impact of both the infection rate and contact rate from contaminated surfaces. These rates are considered in system (2.1) as β and β_e, respectively. The environmental transmission has an impact ($R_e = 0.1713$) of around 7.6% of the total reproduction number ($R_0 = 2.2582$) in transmission of coronavirus in India. Impact of environmental transmission is determined using the simulation of the system (2.1) for distinct values of parameter β_e. Figure 6 I, II, III, IV shows active, asymptomatic, exposed, and symptomatic infectious for distinct values of the parameter β_e. Figure 6 I, II, III and IV shows that infectious individual increase with the increase in the parameter β_e. Figure 7 I, II represents confirmed and death cases, respectively. It is observed that confirmed and death cases continue to increase with the increase in the parameter β_e.

5 Conclusions

As in the third week of April 2021, India has been faced the second wave of epidemic and mainly affected through community transmissions, super-spreader events, etc., in comparison with the first wave in India and many other countries that time. The Indian government made many efforts to flatten the novel coronavirus curve to control the number of infectious by extending the medical facility. We have developed a mathematical model by extending SEIAQRDT (Kumari et al. 2021a) model to introduce a new compartment corresponding to environment transmission factors. In addition to this, the parameters like death rate and requirement rate have been incorporated. The mathematical analysis of the model has been presented, and it is concluded that DFE is locally asymptomatically and globally stable; on the other hand, EE point is locally asymptomatically stable. The comparison between real data and simulated data using proposed model has been done. Normalized root mean square error (NRSME) has been calculated for the real data of India and predicated results to demonstrate the efficiency of considered model. The NRSME corresponding to real and predicated data for India is 0.0075 which shows the efficacy of proposed model. The impact of environmental transmission and protection rate is anticipated. It is noticed that environmental transmission has an impact of around 7.6% to total spread of coronavirus in India. Thus, the effect of environmental transmission in India is moderate. In correspondence to previous studies (Ngonghala et al. 2020; Iboi et al. 2020), this study also proposed that care must be taken while relaxing the novel coronavirus alerts to avoid further waves in future. Furthermore, this model can be extended by introducing the role of vaccination, new treatment tools and the effect of other disease on COVID-19.

Acknowledgements Harendra Pal Singh is supported by the Faculty Research Programme Grant 2021–22 from IoE, University of Delhi, India.

Author Contribution All authors contributed to the study conception and design. Material preparation and analysis were performed by P K and H P S. The first draft of the manuscript was written by P K, and all authors commented on previous versions of the manuscript. All authors read and approved the final manuscript.

Funding The corresponding author would like to thank IoE, University of Delhi, India, for financial support (Ref. No./IoE/2021/12/FRP).

Data Availability All data generated during this study are included in this article.This article does not contain any studies with human participants or animals performed by any of the authors.

Declarations

Conflict of interest The authors declare that they have no conflict of interest.

References

Alqarni MS, Alghamdi M, Muhammad T, Alshomrani AS, Khan MA (2020) Mathematical modeling for novel coronavirus (COVID-19) and control. Numer Methods Partial Differ Equ 38(4):760–776

Asif M, Khan ZA, Haider N, Al-Mdallal Q (2020) Numerical simulation for solution of SEIR models by meshless and finite difference methods. Chaos Solitons Fractals 141:110340

Babaei A, Ahmadi M, Jafari H, Liya A (2021) A mathematical model to examine the effect of quarantine on the spread of coronavirus. Chaos Solitons Fractals 142:110418

Beghami W, Maayah B, Bushnaq S et al (2022) The laplace optimized decomposition method for solving systems of partial differential equations of fractional order. Int J Appl Comput Math 8:52. https://doi.org/10.1007/s40819-022-01256-x

Castillo-Chavez C, Song B (2004) Dynamical models of tuberculosis and their applications. Math Biosci Eng 1(2):361

Castillo-Chavez C, Feng Z, Huang W (2002) On the computation of $R\sim 0$ and its role in global stability. IMA Vol Math Its Appl 125:229–250

Cheynet E (2020) Generalized SEIR Epidic Model (fitting and computation). Zenodo. https://doi.org/10.5281/ZENODO.3911854

Covid19 India (2021) Available from: https://www.covid19india.org/. (Accessed: August 08, 2021)

de León UAP, Pérez ÁG, Avila-Vales E (2020) An SEIARD epidemic model for COVID-19 in Mexico: mathematical analysis and state-level forecast. Chaos Solitons Fractals 140:110165

Djilali S, Ghanbari B (2020) Coronavirus pandemic: a predictive analysis of the peak outbreak epidemic in South Africa, Turkey, and Brazil. Chaos Solitons Fractals 138:109971

Dowell SF, Simmerman JM, Erdman DD, Wu JSJ, Chaovavanich A, Javadi M, Yang JY, Anderson LJ, Tong S, Ho MS (2004) Severe acute respiratory syndrome coronavirus on hospital surfaces. Clin Infect Dis 39(5):652–657

Elmojtaba I M, Al-Musalhi F, Al-Ghassani A, Al-Salti N (2020) Investigating the role of environmental transmission in COVID-19 Dynamics: a mathematical model Based Study

Fu S, Milne G (2003) Epidemic modelling using cellular automata. In: Proceedings of the Australian conference on artificial life

Garba SM, Lubuma JMS, Tsanou B (2020) Modeling the transmission dynamics of the COVID-19 Pandemic in South Africa. Math Biosci 328:108441

Giordano G, Blanchini F, Bruno R, Colaneri P, Di Filippo A, Di Matteo A, Colaneri M (2020) Modelling the COVID-19 epidemic and implementation of population-wide interventions in Italy. Nat Med 26(6):855–860

Gralinski LE, Menachery VD (2020) Return of the coronavirus: 2019-nCoV. Viruses 12(2):135

Gumel AB, Ruan S, Day T, Watmough J, Brauer F, Van den Driessche P, Sahai BM (2004) Modelling strategies for controlling SARS outbreaks. Proc R Soc Lond B 271(1554):2223–2232

Gunia A, (2020) Will COVID-19 ever go away? Time (Gunia-20)

Iboi EA, Sharomi OO, Ngonghala CN, Gumel AB (2020) Mathematical modeling and analysis of COVID-19 pandemic in Nigeria. MedRxiv 5:293

Ivorra B, Ferrández MR, Vela-Pérez M, Ramos AM (2020) Mathematical modeling of the spread of the coronavirus disease 2019 (COVID-19) taking into account the undetected infections The case of China. Commun Nonlinear Sci Numer Simul 88:105303

Ji JS (2020) Origins of MERS-CoV, and lessons for 2019-nCoV. The Lancet Planet Health 4(3):e93

Kampf G, Todt D, Pfaender S, Steinmann E (2020) Persistence of coronaviruses on inanimate surfaces and their inactivation with biocidal agents. J Hosp Infect 104(3):246–251

Kizito M, Tumwiine J (2018) A mathematical model of treatment and vaccination interventions of pneumococcal pneumonia infection dynamics. J Appl Math 2018:1–16

Krishna MV, Prakash J (2020) Mathematical modelling on phase-based transmissibility of Coronavirus. Infect Dis Model 5:375–385

Kumari P, Singh HP, Singh S (2021a) SEIAQRDT model for the spread of novel coronavirus (COVID-19): A case study in India. Appl Intell 51(5):2818–2837

Kumari P, Singh S, Singh HP (2021b) Bifurcation and stability analysis of glucose-insulin regulatory system in the presence of β-cells. Iran J Sci Technol Trans Sci 45(5):1743–1756

Liu QX, Jin Z, Liu MX (2006) Spatial organization and evolution period of the epidemic model using cellular automata. Phys Rev E 74(3):031110

Milne G, Fermanis C, Johnston P (2008) A mobility model for classical swine fever in feral pig populations. Vet Res 39(6):53–53

Momani S, Abu Arqub O, Maayah B (2020a) Piecewise optimal fractional reproducing kernel solution and convergence analysis for the Atangana–Baleanu–Caputo model of the Lienard's equation. Fractals 28(08):2040007. https://doi.org/10.1142/S0218348X20400071

Momani S, Maayah B, Arqub OA (2020b) The reproducing kernel algorithm for numerical solution of Van der Pol damping model in view of the Atangana-Baleanu fractional approach. Fractals 28(08):2040010. https://doi.org/10.1142/S0218348X20400101

Murray J (1993) Mathematical Biology. Springer, Berlin

Ndaïrou F, Area I, Nieto JJ, Torres DF (2020) Mathematical modeling of COVID-19 transmission dynamics with a case study of Wuhan. Chaos, Solitons Fractals 135:109846

Ngonghala CN, Iboi E, Eikenberry S, Scotch M, MacIntyre CR, Bonds MH, Gumel AB (2020) Mathematical assessment of the impact of non-pharmaceutical interventions on curtailing the 2019 novel Coronavirus. Math Biosci 325:108364

Ong SWX, Tan YK, Chia PY, Lee TH, Ng OT, Wong MSY, Marimuthu K (2020) Air, surface environmental, and personal protective equipment contamination by severe acute respiratory syndrome coronavirus 2 (SARS-CoV-2) from a symptomatic patient. JAMA 323(16):1610–1612

Otter JA, Donskey C, Yezli S, Douthwaite S, Goldenberg S, Weber DJ (2016) Transmission of SARS and MERS coronaviruses and influenza virus in healthcare settings: the possible role of dry surface contamination. J Hosp Infect 92(3):235–250

Oud MAA, Ali A, Alrabaiah H, Ullah S, Khan MA, Islam S (2021) A fractional order mathematical model for COVID-19 dynamics with quarantine, isolation, and environmental viral load. Adv Difference Equ 2021(1):1–19

Pfeifer B, Kugler K, Tejada MM, Baumgartner C, Seger M, Osl M, Netzer M, Handler M, Dander A, Wurz M, Graber A, Tilg B (2008) A cellular automaton framework for infectious disease spread simulation. Open Med Inform J 2:70

Rabah AB, Momani S, Arqub OA (2022) The B-spline collocation method for solving conformable initial value problems of non-singular and singular types. Alex Eng J 61(2):963–974. https://doi.org/10.1016/j.aej.2021.06.011

Rogers A (2020) The Asian countries that beat COVID-19 have to do it again. WIRED (Wired) (Accessed on April 13, 2020)

Roosa K, Lee Y, Luo R, Kirpich A, Rothenberg R, Hyman JM, YanChowell PGB (2020) Real-time forecasts of the COVID-19 epidemic in China from February 5th to February 24th, 2020. Infect Dis Model 5:256–263

Samui P, Mondal J, Khajanchi S (2020) A mathematical model for COVID-19 transmission dynamics with a case study of India. Chaos Solitons Fractals 140:110173

Seladi-Schulman J (2020) How long does the coronavirus leave on different surfaces? Healthline (Seladi-20). (Accessed 29 April 2020)

Sweilam NH, Al-Mekhlafi SM, Baleanu D (2020) A hybrid fractional optimal control for a novel Coronavirus (2019-nCov) mathematical model. J Adv Res 32:149–160

Usaini S, Hassan AS, Garba SM, Lubuma JS (2019) Modeling the transmission dynamics of the Middle East Respiratory Syndrome Coronavirus (MERS-CoV) with latent immigrants. J Interdiscip Math 22(6):903–930

White SH, Del Rey AM, Sánchez GR (2007) Modeling epidemics using cellular automata. Appl Math Comput 186(1):193–202

WHO (2020) WHO Director-General's opening remarks at the media briefing on COVID-19, 11 March 2020, URL = https://www.who.int/dg/speeches/detail/who-director-general-sopening-remarks-at-the-media-briefing-on-covid-19—11-march-2020

World Health Assembly (2013) Global overview of an emerging novel coronavirus (MERS-CoV) (WorldHealthAssembly-20)

World Health Organization (WHO) Coronavirus disease (COVID 19) pandemic. Available from: https://www.who.int/emergencies/diseases/novel-coronavirus-2019/technical-guidance2020. (Accessed: July 2021)

World Health Organization, Situation Report - 166, 2020.

Worldometer 2020a (Worldometer-20). Available from: https://www.worldometers.info/coronavirus/world (Accessed: August 26, 2021)

Worldometer 2020b (Worldometer-20). Available from: https://www.worldometers.info/coronavirus/indiad (Accessed: August 26, 2021)

Wu JT, Leung K, Leung GM (2020) Nowcasting and forecasting the potential domestic and international spread of the 2019-nCoV outbreak originating in Wuhan, China: a modelling study. The Lancet 395(10225):689–697

Yang C, Wang J (2020) A mathematical model for the novel coronavirus epidemic in Wuhan. China Math Biosci Eng MBE 17(3):2708

Springer Nature or its licensor (e.g. a society or other partner) holds exclusive rights to this article under a publishing agreement with the author(s) or other rightsholder(s); author self-archiving of the accepted manuscript version of this article is solely governed by the terms of such publishing agreement and applicable law.